PAPER

A promising cation of 4-aminofurazan-3-carboxylic acid amidrazone in desensitizing energetic materials†

Jichuan Zhang,‡[ac] Zhenyuan Wang,‡[b] Yunhao Hsieh,[b] Binshen Wang,[b] Haifeng Huang, [ID][a] Jun Yang [ID] *[a] and Jiaheng Zhang [ID] *[bc]

For the development of energetic materials, insensitive compounds have attracted considerable attention due to their improved safety and lower cost than those of sensitive energetic compounds during production, transportation, and application. In this study, insensitive 4-aminofurazan-3-carboxylic acid amidrazone was used as a cation to obtain four derivatives which were determined by X-ray single crystal diffraction. It is interesting to note that all four derivatives are insensitive to impact and friction, while the velocities of detonation for derivatives are superior to that of insensitive TATB (1,3,5-triamino-2,4,6-trinitrobenzene). Multi-factors analysis shows that the cation of 4-aminofurazan-3-carboxylic acid amidrazone is a promising furazan-based cation in desensitizing energetic compounds.

Introduction

Since the discovery of dynamite by Alfred Bernhard Nobel, energetic compounds with a considerable amount of stored chemical energy have played a crucial role in the civil and military defence industries.[1] During the development and investigation of new-generation energetic compounds, insensitive energetic materials have attracted extensive attention as it can decrease the cost and risk greatly compared to those of less sensitive or sensitive compounds during the production, transportation, and application.[2] Several strategies were employed to design insensitive compounds, such as introducing insensitive groups (NH_2, CH_3) to energetic backbone, assembly of energetic metal–organic frameworks, layer–layer packing, forming strong hydrogen bonds, as well as the combination of the above multi-factors.[3]

[a]CAS Key Laboratory of Energy Regulation Materials, Shanghai Institute of Organic Chemistry, Chinese Academy of Sciences, 345 Lingling Road, Shanghai, 200032, China. E-mail: yangj@sioc.ac.cn

[b]School of Material Sciences and Engineering, Harbin Institute of Technology, Shenzhen, 518055, China. E-mail: zhangjiaheng@hit.edu.cn

[c]Biomaterials Research Center, Zhuhai Institute of Advanced Technology, Chinese Academy of Sciences, Zhuhai, 519003, China

‡ These authors contributed equally to this work, and they did the majority of this work.

Hydrogen bonds (H-bonds) are divided into two categories, intramolecular and intermolecular H-bonds,[4] which play a significant role in desensitization of energetic compounds. In general, intramolecular H-bonds are the stronger one, this is due to (1) intramolecular H-bonds connect donator and acceptor in a molecule, which can make the molecule considerably more firm than those contain intramolecular H-bonds; and (2) intramolecular H-bonds could enhance the conjugation effect of the molecule, and result in a planar molecule, which are usually less sensitive than nonplanar energetic compounds, such as the classic insensitive compounds, TATB, LLM-116, and FOX-7, which are obviously less sensitive than their derivatives.[3b,5] However, for energetic materials, most of the reported strong intramolecular H-bonds are N–H⋯O, the intramolecular H-bonds of N–H⋯N are reported rarely.[4a] In addition, intermolecular H-bonds help form infinite networks as it may also cause denser packing which reduces the amount of free space in the crystal lattice, and thereby decreasing sensitivity.[6]

Nitrogen-rich heterocyclic rings have drawn extensive interest in the past two decades due to their high heat of formation and nitrogen content.[7] Comparing with these general known heterocyclic rings, 1,2,5-oxadiazole ring (furazan) exhibits promising performance due to its higher density, and better oxygen balance than pyrazole and 1,2,4-triazole. In addition, furazan also displays higher heat of formation than 1,2,4-oxadiazole ring.[8] Some derivatives with furazan ring show huge potential as new generation energetic materials.[9] The cations of furazan based energetic salts are inorganic cations, such as ammonium, hydronium, and hydroxylammonium. Although some azole rings have been employed as energetic

cations while the furazan ring as energetic cation has been studied rarely.

4-Aminofurazan-3-carboxylic acid amidrazone which is insensitive to impact and friction was synthesized and characterized in this work. Single crystal structure shows that it contains not only intermolecular H-bonds, but also strong N···H–N intramolecular H-bonds. If these H-bonds were still in its derivatives, the sensitivities of its derivatives would possibly be decreased greatly. Now, four derivatives (**1a**: nitrate; **1b**: 1*H*,1*H*-5,5-bitetrazole-1,1-diolate; **1c**: 3-nitramino-4-tetrazolefurazanate; **1d**: 3,4-dinitramino-furazanate) of 4-aminofurazan-3-carboxylic acid amidrazone were synthesized and characterized (Scheme 1). Their crystal structures, energetic properties, and sensitivities were investigated comprehensively.

Results and discussion

Synthesis and single crystal X-ray structures

Based on the previous study[10] and the synthetic route shown in Fig. 1, 4-(1,2,4-oxadiazol-3-yl)furazan-3-amine, a luminous yellow solid, was synthesized in high yield (85%), followed by treatment with 80% of hydrazine hydrate in methanol at 50 °C for 1 h while 4-aminofurazan-3-carboxylic acid amidrazone (1) exhibits as a brown solid. Compound **1** was recrystallized from water, and then it reacted with dilute HNO_3 in methanol, after the solvent was removed, affording **1a·H$_2$O**. **1** reacted with HCl, affording an amidrazone of 4-aminofurazan-3-carboxylic acid chloride salt and then chloride salt of **1** react with the corresponding silver salts of **1b–1d** in water for 30 min, **1b–1d** were obtained after filtration, evaporation. Finally, these four salts were obtained after recrystallization from mixture of water and methanol, and drying, respectively.

Compound **1** was crystalized from water in the monoclinic space group $P12_1/c1$ with a density of 1.627 g cm^{-3} at 173 K (Table S1†), as well as eight molecules in a unit cell ($Z = 8$, Fig. 2a). Five intramolecular H-bonds were observed in **1**: N9–H9B···N11, N4–H4A···N1, N3–H3B···N5, N10–H10A···N12 and N10–H10B···N7. The corresponding hydrogen···acceptor (H···A) distances were 2.215 Å, 2.332 Å, 2.410 Å, 2.425 Å and 2.410 Å (Table 1), respectively. Comparing to the reported N–H···N intramolecular H-bonds (H···A > 2.52 Å),[4a] the intramolecular H-bonds in **1** are shorter and stronger while the amount of intramolecular H-bonds is greater. The intramolecular H-bonds resulted in coplanar structure of all the non-hydrogen atoms of
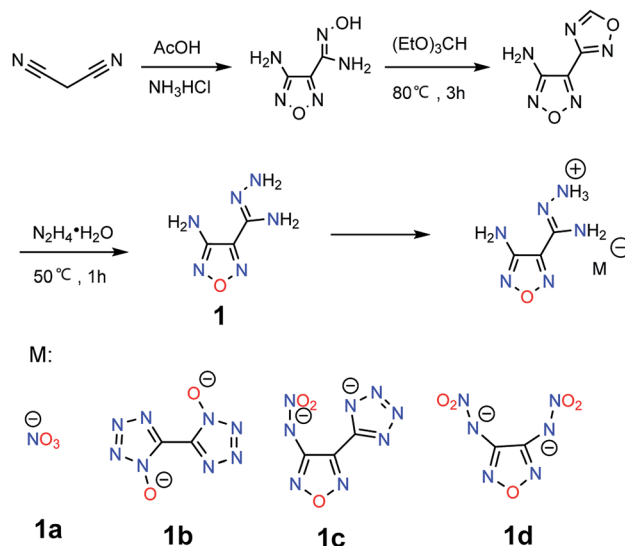

Fig. 1 Synthetic route of compounds **1** and **1a–1d**.

1 (Fig. 4a and Tables S1 and S2†). Apart from intramolecular H-bonds, five intermolecular H-bonds were also observed, with lengths of 2.209, 2.219, 2.335, 2.425, and 2.465 Å, respectively (Table S6†). Finally, the crystal structure was connected by these intermolecular H-bonds, forming an infinite three-dimensional (3D) network (Fig. S6 and 7†).

Compound **1a·H$_2$O** was crystalized as a colourless block crystal in the orthorhombic *Pbca* space group, with eight NO_3 anions, eight amidrazone of 4-aminofurazan-3-carboxylic acid cations, and eight water molecules in each unit cell ($Z = 8$, Fig. 2b). The crystal density of **1a·H$_2$O** was 1.64 g cm^{-3} at room temperature. It is interesting that the intramolecular H-bonds still exist in **1a·H$_2$O**, and two intramolecular H-bonds (N3–H3B···N4) and (N6–H6A···N1) are observed. The hydrogen··· acceptor (H···A) distance are 2.295 Å and 2.382 Å, respectively. The intramolecular H-bonds make the atoms of cation and oxygen from water molecules close to coplanar (Fig. 4b and Table S3†). In addition, seven intermolecular H-bonds were observed in a unit cell, and the lengths of their H···A were 1.881, 2.010, 2.077, 2.082, 2.198, 2.203 and 2.209 Å, respectively. These intermolecular H-bonds connect NO_3 anions, water molecules as well as amidrazone of 4-aminofurazan-3-carboxylic acid cations forming an infinite 3D network structure (Fig. S8 and 9†).
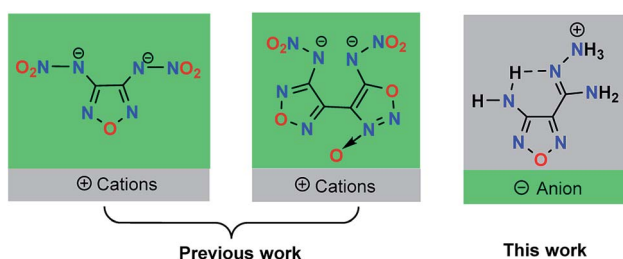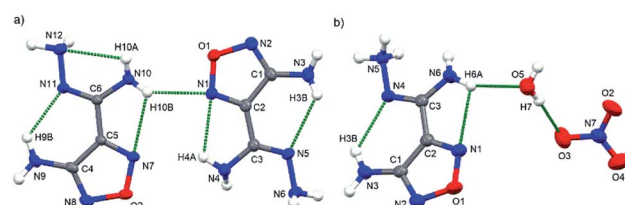

Scheme 1 Energetic salts based on furazan-ring.

Fig. 2 Single crystal structures and hydrogen bonds of **1** (a) and **1a·H$_2$O** (b) (hydrogen bonds: green dash line).
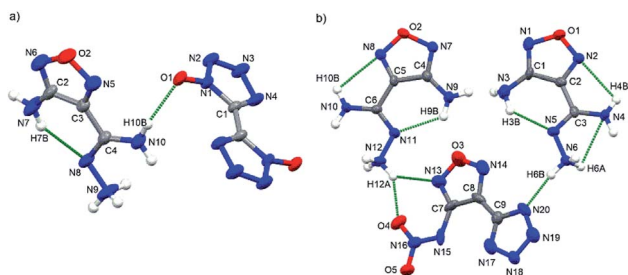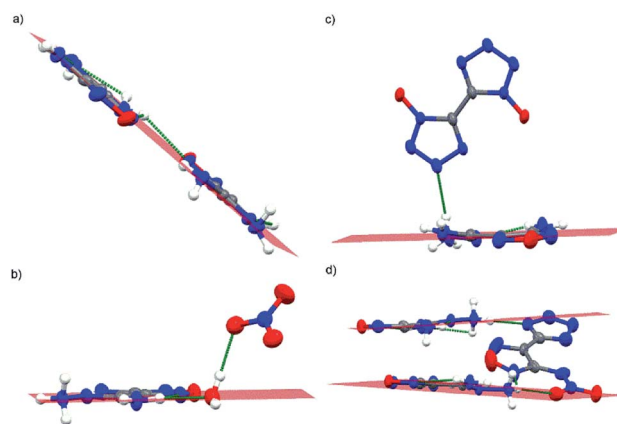
Table 1 Intramolecular hydrogen bonding distances (Å) and angle (°) for compounds **1**, **1a·H₂O** and **1b–1c**

Comp	D–H⋯A	D–H (Å)	H⋯A (Å)	D–H⋯A (Å)	<DHA (°)
1	N3–H3B⋯N5	0.883	2.410	2.930	118.06
	N9–H9⋯N11	0.881	2.215	2.814	124.91
	N4–H4A⋯N1	0.884	2.332	2.798	112.97
	N10–H10B⋯N7	0.886	2.425	2.799	105.78
	N10–H10A⋯N12	0.886	2.419	2.699	98.72
1a·H₂O	N3–H3B⋯N4	0.805	2.295	2.847	126.37
	N6–H6A⋯N1	0.861	2.382	2.771	107.89
1b	N7–H7B⋯N8	0.859	2.269	2.826	122.54
1c	N3–H3B⋯N5	0.882	2.168	2.855	134.36
	N9–H9B⋯N11	0.880	2.250	2.828	123.02
	N4–H4B⋯N2	0.880	2.455	2.770	102.31
	N6–H6A⋯N4	0.910	2.491	2.727	95.12
	N10–H10B⋯N8	0.880	2.471	2.794	102.30

Fig. 4 Coplanar structures of **1** and cations in various compounds ((a): compound **1**; (b): compound **1a**; (c): compound **1b**; (d): compound **1c**).

1b was crystalized as a colourless block in the monoclinic $P2_1/c$ space group accompanied by four anions and eight cations in a unit cell (Fig. 3a). Its density was 1.70 g cm^{-3} at room temperature. The structure of **1b** is similar to **1a** as **1b** contains intramolecular H-bond (N7–H7B⋯N8) in the cation while the hydrogen⋯acceptor (H7B⋯N8) distance was 2.275 Å. The intramolecular H-bonds cause all the non-hydrogen atoms of the cation to coplanar (Fig. 4c and Table S4†). Moreover, a large amount of intermolecular H-bonds was observed throughout the intermolecular H-bonds connected 3D crystal structure (Fig. S10 and 11†), with lengths of 1.892, 2.048, 2.119, 2.303, 2.271, and 2.489 Å, respectively.

1c was crystalized in the monoclinic $P1n1$ space group, with two anions and four cations in a unit cell ($Z = 2$, Fig. 3b). Similar to **1**, five intramolecular H-bonds (N3–H3B⋯N5, N9–H9B⋯N11, N4–H4B⋯N2, N6–H6A⋯N4 and N10–H10B⋯N8 respectively) were observed in two neighbouring cations, and their corresponding hydrogen⋯acceptor (H3B⋯N5, H9B⋯N11) lengths were 2.168 Å, 2.250 Å, 2.455 Å, 2.471 Å and 2.491 Å, respectively, which are more stronger than those in **1**. The intramolecular H-bonds make cation almost coplanar (Fig. 4d and Table S5†). Further, as many as 13 intermolecular H-bonds throughout the crystal were observed, and the hydrogen⋯acceptor (H⋯A) lengths of these intermolecular H-bonds were 1.928, 1.983, 2.030, 2.060, 2.120, 2.183, 2.193, 2.295, 2.311, 2.355, 2.457, 2.491 and 2.499 Å, respectively. The crystal

structure was connected by these 13 intermolecular H-bonds, forming an infinite 3D network (Fig. S12 and 13†).

To conclude, these N–H⋯N intramolecular H-bonds caused all of the non-hydrogen atoms in the neutral compound and cations coplanar (Fig. 4). The hydrogen⋯acceptor (H⋯A) distance of these intramolecular H-bonds ranged from 2.168 Å to 2.491 Å; they are not only shorter than those reported N–H⋯N intramolecular H-bonds (>2.52 Å), but also shorter than most of those N–H⋯N intermolecular H-bonds (H⋯A: 2.187–2.345 Å).[4a,11] Hence, these strong intramolecular H-bonds permit the close stacking of these compounds. Additionally, the existing large amounts of intermolecular H-bonds of the corresponding compounds allow compounds to pack closely and further led to infinite 3D networks, particularly **1c**, which displayed firm structure as 13 intermolecular H-bonds were observed throughout the crystal.

Thermal stability and sensitivity

Thermal stability is a crucial factor for energetic compounds: the higher the decomposition temperature, the safer the energetic compounds. Thermogravimetric analysis-differential scanning calorimetry (DSC, 5 °C min^{-1}) was employed to characterize the thermal stability of all five compounds prepared in this study. The decomposition temperatures (on set) of **1** was 183.4 °C, while the disintegration temperature of **1a–1d** were 133.0, 184.9, 183.3, and 198.5 °C (Fig. S1–S5†), respectively. The decomposition temperatures of four compounds, **1**, **1b**, **1c** and **1d**, were greater than 180 °C.

All five samples were examined by the Fall-hammer and Friction apparatus and all of them exhibited insensitivity (IS >

Fig. 3 Single crystal structures and hydrogen bonds of **1b** (a) and **1c** (b) (hydrogen bonds: green dash line).

Table 2 The percentage of O–H and N–H week interactions in **1** and **1a·H₂O**, **1b–1c**

Crystal	1	1a·H₂O	1b	1c
O–H (%)	13.2	53.1	23.4	15.7
N–H (%)	35.0	15.4	38.4	38.2

40 J, FS > 360 N) to stimulation *via* impact and friction.[19] Hence, it is beneficial to investigate the insensitivity of these compounds. In this study, all crystals prepared contain N–H⋯N intramolecular H-bonds. As comparing examples with **1a**, 3,5-diamino-1,2,4-triazole, 4,4′,5,5′-tetraamino-3,3′-bis-1,2,4-triazole and 3-methyl-1-amino-1,2,3-triazole are insensitive. The impact and friction sensitivities of 3,5-diamino-1,2,4-triazole nitrate salts are 40 J and 288 N, respectively, and the impact sensitivities of 3-methyl-1-amino-1,2,3-triazole nitrate and 4,4′,5,5′-tetraamino-3,3′-bis-1,2,4-triazole nitrate are 28.9 J and 15 J, respectively, which are obviously more sensitive than those of **1a**,[12] which would possibly result from the strong intramolecular H-bonds, and large amount of intermolecular H-bonds in the structures. Similarly, compounds **1b** and **1c** were less sensitive than the energetic compounds based on 5,5′-dihydrobistetrazole and 3-nitramino-4-tetrazolefurazan.[9d,13] Thus far, all compounds based on 3,4-di(nitramino)furazan were sensitive; hence, **1d** can offer a new route to desensitize compounds of 3,4-di(nitramino)furazan.[9a]

In general, the "soft" O–H and N–H interactions are conducive to stabilizing the crystal structure by absorbing the mechanic stimuli.[14] In this study, Hirshfeld surfaces[15] were employed to analyse the weak interactions of the obtained compounds. As shown in Table 2, the percentage of O–H weak interactions in **1** and **1a·H₂O**, **1b–1c** are 13.2%, 53.1%, 23.4% and 15.7%, respectively, while the percentage of N–H weak interactions in **1**, **1a·H₂O** and **1b–1c** are 35.0%, 15.4%, 38.4%, and 38.2%, respectively. The proportion of N–H weak interactions is higher than O–H weak interactions except **1a·H₂O**, which may due to more O atoms provided by NO_3 anion and H_2O in **1a·H₂O**. The strength of N–H weak interactions in the case of **1** and **1c** are also higher than the strength of O–H weak interactions as shown in Fig. 5 (Fig. S14†). The investigation of weak interactions displays that the large portions of N–H weak interactions are possibly also helpful in decreasing sensitivities.

Detonation properties

To examine the energetic properties of **1** and its derivatives, the heat formation for **1** and its corresponding anion were determined by the isodesmic reaction approach (see ESI†). The computation was performed using the Gaussian 03 suite of programs.[17] The heat formation for **1** and **1a–1d** were 329.1, 208.2, 1507.2, 1432.5, and 1206.1 kJ mol⁻¹, respectively (Table 3). The detonation properties of all new compounds were calculated by EXPLO5 6.01 code with the calculated enthalpies of formation and the measured densities.[18] The detonation velocities and pressures of **1** and **1a–1d** were 7999, 8455, 8680, 8249, and 8541 m s⁻¹ and 22.20, 27.73, 28.77, 25.57, and 28.42 GPa (Table 2), respectively. The detonation properties of all the compounds were greater than that of TNT; especially, the detonation velocity of **1b**, which exhibited the best detonation performance, was 8680 m s⁻¹. This was greater than LLM-116 and comparable to that of RDX. The detonation velocity of **1d** was greater than that of TATB and comparable to that of LLM-116. Samples **1a**, **1b**, and **1d** demonstrated immense
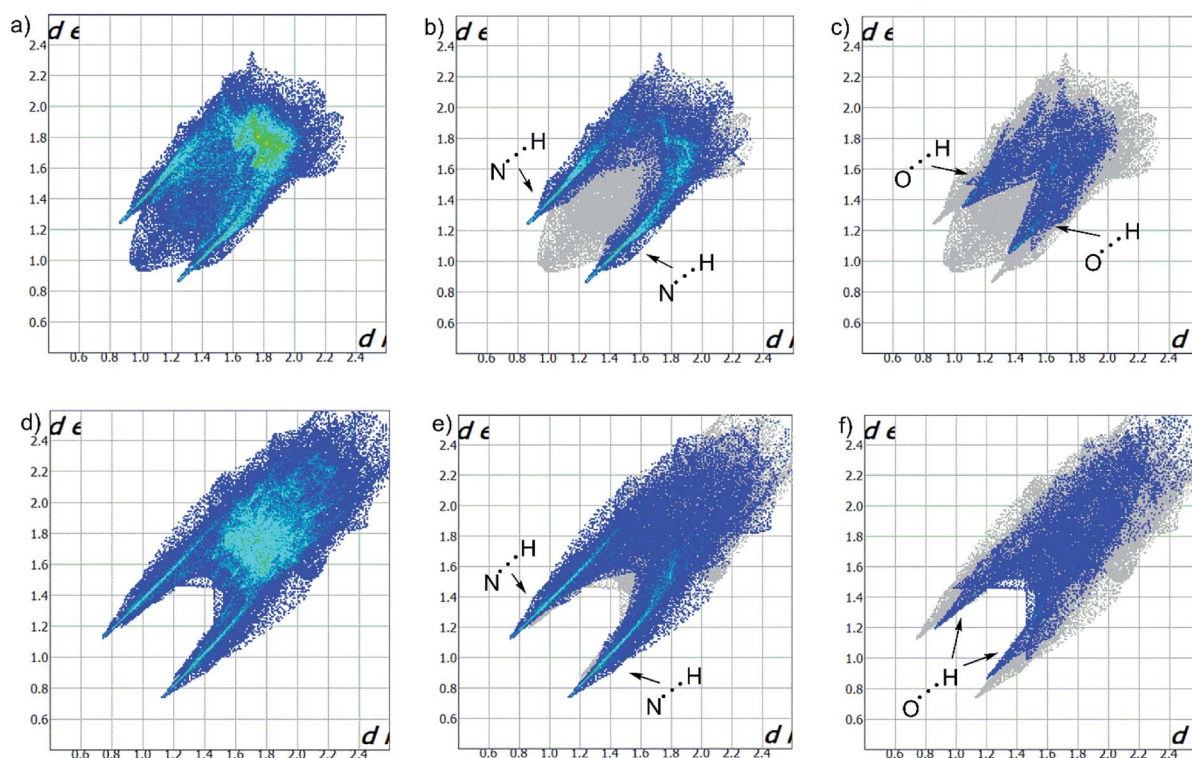

Fig. 5 (a) The total weak interactions of **1**; (b) the N–H weak interactions of **1**; (c) the O–H weak interactions of **1**; (d) the total weak interactions of **1c**; (e) the N–H weak interactions of **1c**; (f) the O–H weak interactions of **1c**.

Table 3   Physical properties of all compounds based on the amidrazone of 4-aminofurazan-3-carboxylic acid

Comp.	$T_m{}^a$ (°C)	$T_d{}^{a\ b}$ (°C)	$d^{b\ c}$ (g cm^{-3})	$\Delta_f H^{c\ d}$ (kJ mol^{-1})	$V_d{}^{d\ e}$ (m s^{-1})	$P^{e\ f}$ (Gpa)	IS$^{f\ g}$ (J)	FS$^{g\ h}$ (N)
1	167.3	198.4	1.60	329.05	7999	22.20	>40	>360
1a	128.5	133	1.68	208.2	8455	27.73	>40	>360
1b	81.6	184.9	1.70	1507.2	8680	28.77	>40	>360
1c	85.7	183.3	1.64	1432.5	8249	25.57	>40	>360
1d	106.4	198.5	1.68	1206.06	8541	28.42	>40	>360
TATB^i	—	360	1.93	−154.2/−0.60	8114	31.2	>40	>360
LLM-116^i	—	178	1.90	96.3/0.56	8573	34.2	>40	>360
RDX^i	—	205	1.81	80/0.36	8795	34.9	7.4	120
TNT^i	81	295	1.65	−67.0/−0.30	6881	19.5	15	353

^{a} Melting point. ^{b} Temperature of decomposition (onset). ^{c} Density measured by using a gas pycnometer at 25 °C. ^{d} Calculated molar enthalpy of formation in the solid state. ^{e} Calculated detonation velocity. ^{f} Calculated detonation pressure. ^{g} Impact sensitivity. ^{h} Friction sensitivity. ^{i} Ref. 3a and 16.

applications as alternatives to traditional classic compounds as they exhibited moderate detonation velocities at an insensitive level.

Conclusions

Insensitive 4-aminofurazan-3-carboxylic acid amidrazone (**1**) was synthesized, and then its four derivatives (**1a–1d**) were prepared and characterized. It is interesting that all four derivatives are insensitive to impact and friction, which were resulted from the combination of strong N–H⋯N intramolecular H-bonds, a large amount of intermolecular H-bonds, and high percentage of weak N–H interactions in these derivatives. In addition, the detonation velocity of compound **1b** is higher than that of LLM-116 and comparable to that of RDX. The detonation velocity of **1d** is greater than that of TATB and comparable to that of LLM-116 demonstrating their promising for applications. In a word, combining multi-stabilizing factors, 4-aminofurazan-3-carboxylic acid amidrazone cation is promising in desensitizing energetic materials.

Experimental

Safety precautions

Although we experienced no difficulties in synthesis and characterization of these materials, proper protective procedures should be followed. All the experiments were carried out in a hood behind a safety shield and face shield, and leather gloves were worn at all times. Caution was exercised at all times during the synthesis, characterization, and handling of any of these materials.

Materials and methods

^{1}H spectra were recorded on a 300 MHz nuclear magnetic resonance spectrometer operating at 300 MHz. ^{13}C NMR spectra were recorded on a 400 MHz nuclear magnetic resonance spectrometer. The solvent were [D6]dimethylsulfoxide ([D6] DMSO) and [D4]methanol ([D4]CH$_3$DO) unless otherwise specified. ^{15}N NMR spectra was recorded on a 400 MHz nuclear magnetic resonance spectrometer operating at 40.5 MHz, the

^{13}C and ^{15}N spectrums were showed from Fig. S15–S20.† Except for single crystal structure determination, before all characterizations (such as thermal stability, sensitivities, element analysis and density, *etc.*), the samples were dried in 60 °C for 6 h, in order to remove the water or moisture of the samples. The melting and decomposition points were recorded on a NETZSCH STA 449F3 equipment at a scan rate of 5 °C min^{-1}, respectively. Infrared spectra were recorded by using KBr pellets. Densities were measured at room temperature using a Micromeritics Accupyc II 1340 gas pycnometer. Elemental analyses were obtained on an Elementar Vario MICRO CUBE (Germany) elemental analyser. Impact and friction-sensitivity measurements were tested by employing a standard BAM Fall-hammer and a BAM friction tester. The acknowledgements come at the end of an article after the conclusions and before the notes and references.

X-ray crystallography

The single-crystal X-ray diffraction data of **1** and **1a–1c** were collected at 293 K using graphite-monochromated MoKα radiation ($\lambda = 0.71073$ Å) using omega scans from a Bruker CCD area detector diffractometer. Data collection and reduction were performed, and the unit cell was initially refined using Bruker SMART software.[20] The reflection data were also corrected for LP factors. The structure was solved by direct methods and refined by a least-squares method on F2 using the Bruker SHELXTL program.[21] In these structures, the value of the Flack parameter did not allow the direction of the polar axis to be determined and Friedel reflections were then merged for the final refinement. Details of the data collection and refinement are given in Table S1.†

Computational method

The gas phase heats of formation for all new neutral compounds and anions were obtained using isodesmic reactions. The geometric optimization and frequency analysis of the structures were calculated using B3LYP function with 6-31+G** basis set. All of the optimized structures were checked to be true local energy minima on the potential energy surface without

imaginary frequencies. Single-point energies based on the optimized structures were calculated at the MP2/6-311++G* set. Atomization energies for the frame molecules or ions were obtained by employing the G2 *ab initio* method. The conversion of gas phase enthalpies to solid phase values for the neutral compounds was done by subtracting the empirical heat of sublimation obtained based on Trouton's rule. Detonation properties of new compounds were calculated by using EXPLO5 program. More calculation details can be found in the ESI.†

Syntheses

According to the literature[10] and synthesis route depicted in Fig. 1, 4-(1,2,4-oxadiazol-3-yl) furazan-3-amine (1.53 g, 10 mmol), a luminous yellow solid, was synthesized with high yield and then treated with 80% hydrazine hydrate in methanol at 50 °C for 30 min. Hence, amidrazone of 4-aminofurazan-3-carboxylic acid (1) was obtained as brown solid with high yield, compound **1** was recrystallized from water, the brown needle-like crystal was obtained, which were used for the synthesis of salts. Yellow solid (1.35 g, 95.3%); ^{1}H NMR (DMSO-d_6): δ 6.39 (NH$_2$, 2H), 5.86 (NH$_2$, 2H), 569 (NH$_2$, 2H) ppm; ^{13}C NMR (DMSO-d_6): δ 155.01, 141.10, 137.13 ppm; ^{15}N NMR ([D4] CH$_3$DO): δ 17.04, −21.67, −122.26, −282.99, −316.14, 335.19 ppm; IR (KBr): ν 3469, 3415, 3353, 3335, 2918, 2848, 1662, 1611, 1555, 1466, 1440, 1405, 1323, 1194, 1144, 1050, 992, 870, 841, 787, 754, 721, 574 cm^{-1}; elemental analysis, calcd (%) for C$_3$H$_6$N$_6$O (142.06): C: 25.35; H: 4.26; N: 59.13; found, C: 25.18; H: 3.98; N: 58.73.

General procedure for the preparation of salts 1a

Compound **1** (0.142 g, 1 mmol) was added to methanol (20 ml) with stirring. HNO$_3$ (5%, 1.23 ml, 1 mmol) was added into the above methanol. The reaction mixture was stirred at room temperature for 30 min followed by evaporation *in vacuo*. The precipitate was collected and recrystalized in the methanol and water. Colourless crystal contains one molecular water on each crystal unit cell (0.18 g, 80.7%), after drying in 60 °C for 6 h, the water in molecular were removed. The ^{1}H NMR (DMSO-d_6): δ 9.29 (NH$_3$, 3H), 8.08 (NH$_2$, 2H), 6.42 (NH$_2$, 2H) ppm; ^{13}C NMR (DMSO-d_6): δ 155.49, 152.77, 140.23 ppm; IR (KBr): ν 3064, 1692, 1545, 1481, 1449, 1351, 1222, 1215, 1150, 1065, 1036, 955, 802, 760, 739, 548 cm^{-1}; elemental analysis, calcd (%) for C$_3$H$_7$N$_7$O$_4$ (204.13): C: 17.65; H: 2.96; N: 48.03; found, C: 17.29; H: 3.06; N: 47.83.

General procedure for the preparation of salts 1b–1d

To a stirring solution of 1·HCl (0.353 mg, 2.0 mmol), the silver compounds (1.0 mmol) of **1b**, **1c** and **1d** were added to the above solutions, respectively. Then, the reaction mixture was stirred at room temperature for 30 min followed by filtration, evaporation. The precipitates were recrystalized from the mixture of methanol and water, respectively. Then dried at 60 °C for 6 h for the next characterisations.

Amidrazone of 4-aminofurazan-3-carboxylic acid 5,5′-bistetrazole-1,1′-diolate (1b)

Yellow solid (0.42 g, 93.1%); ^{1}H NMR (DMSO-d_6): δ 6.92 (NH$_3$, 3H), 6.39 (NH$_2$, 2H), 5.91 (NH$_2$, 2H) ppm; ^{13}C NMR (DMSO-d_6): δ 155.26, 144.56, 140.71, 135.59 ppm; IR (KBr): ν 3064, 1692, 1545, 1481, 1449, 1351, 1222, 1215, 1150, 1065, 1036, 955, 802, 760, 739, 548 cm^{-1}; elemental analysis, calcd (%) for C$_8$H$_{14}$N$_{20}$O$_4$ (454.15): C: 21.15; H: 3.11; N: 61.66; found, C: 20.83; H: 2.76; N: 61.55.

Amidrazone of 4-aminofurazan-3-carboxylic acid 3-nitramino-4-tetrazolefurazanate (1c)

Yellow solid (0.44 g, 91.0%); ^{1}H NMR (DMSO-d_6): δ 7.02 (NH$_2$–NH$_3$, 5H), 6.39 (NH$_2$, 2H) ppm; ^{13}C NMR (DMSO-d_6): δ 158.06, 155.34, 147.64, 145.50, 141.87, 140.72 ppm; IR (KBr): ν 3343, 3287, 3074, 2992, 2887, 1725, 1628, 1575, 1508, 1250, 1140, 1102, 1080, 966, 746 cm^{-1}; elemental analysis, calcd (%) for C$_9$H$_{14}$N$_{20}$O$_5$ (482.15): C: 22.41; H: 2.93; N: 58.08; found, C: 22.07; H: 3.17; N: 57.89.

Amidrazone of 4-aminofurazan-3-carboxylic acid 3,4-dinitraminofurazanate (1d)

Yellow solid (0.43 g, 91.5%); ^{1}H NMR (DMSO-d_6): δ 7.12 (NH$_3$, 3H), 6.92 (NH$_2$, 2H), 6.41 (NH$_2$, 2H) ppm; ^{13}C NMR (DMSO-d_6): δ 155.69, 155.24, 147.65, 141.85, 140.01 ppm; IR (KBr): ν 3466, 3414, 3349, 3269, 3206, 1723, 1647, 1494, 1452, 1361, 1219, 1134, 1072, 962 cm^{-1}; elemental analysis, calcd (%) for C$_8$H$_{14}$N$_{18}$O$_7$ (474.13): C: 20.26; H: 2.98; N: 53.13; found, C: 20.15; H: 2.63; N: 53.40.

Author contributions

Yunhao Hsieh polished this paper. Binshen Wang and Haifeng Huang helped do some calculations for this job. Jun Yang and Jiaheng Zhang provide the idea of this paper together.

Conflicts of interest

The authors declare no competing financial interest.

Acknowledgements

References

1 (a) J. P. Agrawal and R. D. Hodgson, *Organic Chemistry of Explosives*, John Wiley & Sons Ltd, Copyright, 2007; (b) H. Gao and J. M. Shreeve, *Chem. Rev.*, 2011, **111**, 7377–7436.

2 (a) L. Hu, P. Yin, G. Zhao, C. He, G. H. Imler, D. A. Parrish, H. Gao and J. M. Shreeve, *J. Am. Chem. Soc.*, 2018, **140**, 15001–15007; (b) W. Zhang, J. Zhang, M. Deng, X. Qi, F. Nie and Q. Zhang, *Nat. Commun.*, 2017, **8**, 181; (c) Y. Tang, D. Kumar and J. M. Shreeve, *J. Am. Chem. Soc.*, 2017, **139**, 13684–13687; (d) J. Zhang, J. Zhang, D. A. Parrish and J. M. Shreeve, *J. Mater. Chem. A*, 2018, **6**, 22705–22712; (e) Q. Wang, S. Wang, X. Feng, L. Wu, G. Zhang, M. Zhou, B. Wang and L. Yang, *ACS Appl. Mater. Interfaces*, 2017, **9**, 37542–37547; (f) Y. Zhang, H. Gao, Y.-H. Joo and J. M. Shreeve, *Angew. Chem., Int. Ed.*, 2011, **50**, 9554–9562.

3 (a) J. Zhang, J. Zhang, D. A. Parrish and J. M. Shreeve, *J. Mater. Chem. A*, 2018, **6**, 22705–22712; (b) J. Zhang, L. A. Mitchell, D. A. Parrish and J. M. Shreeve, *J. Am. Chem. Soc.*, 2015, **137**, 10532–10535; (c) Y. Wang, Y. Liu, S. Song, Z. Yang, X. Qi, K. Wang, Y. Liu, Q. Zhang and Y. Tian, *Nat. Commun.*, 2018, **9**, 2444; (d) S. Li, Y. Wang, C. Qi, X. Zhao, J. Zhang, S. Zhang and S. Pang, *Angew. Chem., Int. Ed.*, 2013, **52**, 1–6.

4 (a) C. He, P. Yin, L. A. Mitchell, D. A. Parrish and J. M. Shreeve, *Chem. Commun.*, 2016, **52**, 8123–8126; (b) Y. Ma, A. Zhang, C. Zhang, D. Jiang, Y. Zhu and C. Zhang, *Cryst. Growth Des.*, 2014, **14**, 4703–4713.

5 (a) P. A. Pagoria, *Propellants, Explos., Pyrotech.*, 2016, **41**, 452–469; (b) Y. Tang, C. He, G. H. Imler, D. A. Parrish and J. M. Shreeve, *Dalton Trans.*, 2019, **48**, 7677–7684; (c) R. D. Schmidt, G. S. Lee, P. F. Pagoria and A. R. Mitchell, *J. Heterocycl. Chem.*, 2001, **38**, 1227–1230; (d) N. V. Muravyev, A. A. Bragin, K. A. Monogarov, A. S. Nikiforova, A. A. Korlyukov, I. V. Fomenkov, N. I. Shishov and A. N. Pivkina, *Propellants, Explos., Pyrotech.*, 2016, **41**, 999–1005; (e) H. Gao and J. M. Shreeve, *Angew. Chem., Int. Ed.*, 2015, **54**, 6335–6338.

6 T. Brinck, *Green Energetic Materials*, Wiley, 2014.

7 P. Yin, Q. Zhang and J. M. Shreeve, *Acc. Chem. Res.*, 2016, **49**, 4–16.

8 J. Zhang, P. Yin, G. Pan, Z. Wang, J. Zhang, L. A. Mitchell, D. A. Parrish and J. M. Shreeve, *New J. Chem.*, 2019, **43**, 12684–12689.

9 (a) Y. Tang, J. Zhang, L. A. Mitchell, D. A. Parrish and J. M. Shreeve, *J. Am. Chem. Soc.*, 2015, **137**, 15984–15987; (b) C. He and J. M. Shreeve, *Angew. Chem., Int. Ed.*, 2016, **55**, 772–775; (c) Y. Li, H. Huang, Y. Shi, J. Yang, R. Pan and X. Lin, *Chem.–Eur. J.*, 2017, **23**, 7353–7360; (d) H. Huang, Y. Shi, Y. Li, Y. Liu and J. Yang, *RSC Adv.*, 2016, **6**, 64568–64574.

10 (a) A. I. Stepanov, V. S. Sannikov, D. V. Dashko, A. G. Roslyakov, A. A. Astrat'ev and E. V. Stepanova, *Chem. Heterocycl. Compd.*, 2015, **51**, 350–360; (b) A. I. Stepanov, V. S. Sannikov, D. V. Dashko, A. G. Roslyakov, A. A. Astrat'yev, E. V. Stepanova, Z. G. Aliev, T. K. Goncharov and S. M. Aldoshin, *Chem. Heterocycl. Compd.*, 2017, **53**, 779–785.

11 (a) C. Zhang, C. Sun, B. Hu, C. Yu and M. Lu, *Science*, 2017, **355**, 374–376; (b) Y. Zhang, Y. Huang, D. A. Parrish and J. M. Shreeve, *J. Mater. Chem.*, 2011, **21**, 6891–6897.

12 (a) Q. Lin, Y. Li, Y. Li, Z. Wang, W. Liu, C. Qi and S. Pang, *J. Mater. Chem.*, 2012, **22**, 666–674; (b) T. M. Klapötke, P. C. Schmid, S. Schnell and J. Stierstorfer, *J. Mater. Chem. A*, 2015, **3**, 2658–2668.

13 N. Fischer, T. M. Klapötke, M. Reymann and J. Stierstorfer, *Eur. J. Inorg. Chem.*, 2013, 2167–2180.

14 (a) C. Y. Zhang, X. G. Xue, Y. F. Cao, Y. Zhou, H. Z. Li, J. H. Zhou and T. Gao, *CrystEngComm*, 2013, **15**, 6837–6844; (b) P. Yin, L. A. Mitchell, D. A. Parrish and J. M. Shreeve, *Chem.–Asian J.*, 2017, **12**, 378–384.

15 M. A. Spackman and D. Jayatilaka, *CrystEngComm*, 2009, **11**, 19–32.

16 P. Yin, J. Zhang, D. A. Parrish and J. M. Shreeve, *J. Mater. Chem. A*, 2015, **3**, 8606–8612.

17 M. J. Frisch, G. W. Trucks, H. B. Schlegel, G. E. Scuseria, M. A. Robb, J. R. Cheeseman, J. A. Montgomery Jr., T. Vreven, K. N. Kudin, J. C. Burant, J. M. Millam, S. S. Iyengar, J. Tomasi, V. Barone, B. Mennucci, M. Cossi, G. Scalmani, N. Rega, G. A. Petersson, H. Nakatsuji, M. Hada, M. Ehara, K. Toyota, R. Fukuda, J. Hasegawa, M. Ishida, T. Nakajima, Y. Honda, O. Kitao, H. Nakai, M. Klene, X. Li, J. E. Knox, H. P. Hratchian, J. B. Cross, V. Bakken, C. Adamo, J. Jaramillo, R. Gomperts, R. E. Stratmann, O. Yazyev, A. J. Austin, R. Cammi, C. Pomelli, J. W. Ochterski, P. Y. Ayala, K. Morokuma, G. A. Voth, P. Salvador, J. J. Rabuck, K. Raghavachari, J. B. Foesman, J. V. Ortiz, Q. Cui, A. G. Baboul, S. Clifford, J. Cioslowski, B. B. Stefanov, A. Lo. G. Liu, P. Piskorz, I. Komaromi, R. L. Martin, D. J. Fox, T. Keith, M. A. Al-Laham, C. Peng, A. Nanayakkara, M. Challacombe, P. M. W. Gill, B. Johnson, W. Chen, M. Wong, C. Gonzalez and J. A. Pople, *Gaussian 03 (Revision E.01)*, Gaussian, Inc, Wallingford CT, 2004.

18 M. Sucéska, *EXPLO5, Version 6.01*, Brodarski Institute, Zagreb, Croatia, 2013.

19 (a) *13 U. M. Regulations, UN Recommendations on the Transport of Dangerous Goods, Manual of Tests and Criteria*, United Nations Publication, New York, 5th edn, 2009; (b) *13.4.2 Test 3 (a) (ii) BAM Fallhammer*, p. 75; (c) *13.5.1 Test 3 (b) (i) BAM friction apparatus*, p. 104, according to UN recommendations on the transport of dangerous goods: impact, insensitive > 40 J, less sensitive $\geq$ 35 J, sensitive $\geq$ 4 J, very sensitive $\leq$ 3 J; friction, insensitive > 360 N, less sensitive 360 N, 80 N < sensitive < 360 N, very sensitive < 80 N, extremely sensitive < 10 N.

20 *Bruker SAINT (SADABS), v2008/1*, Bruker AXS Inc., Madison, Wisconsin, 2008.

21 *Bruker SHELXTL, v2008/1*, Bruker AXS Inc., Madison, Wisconsin, 2008.